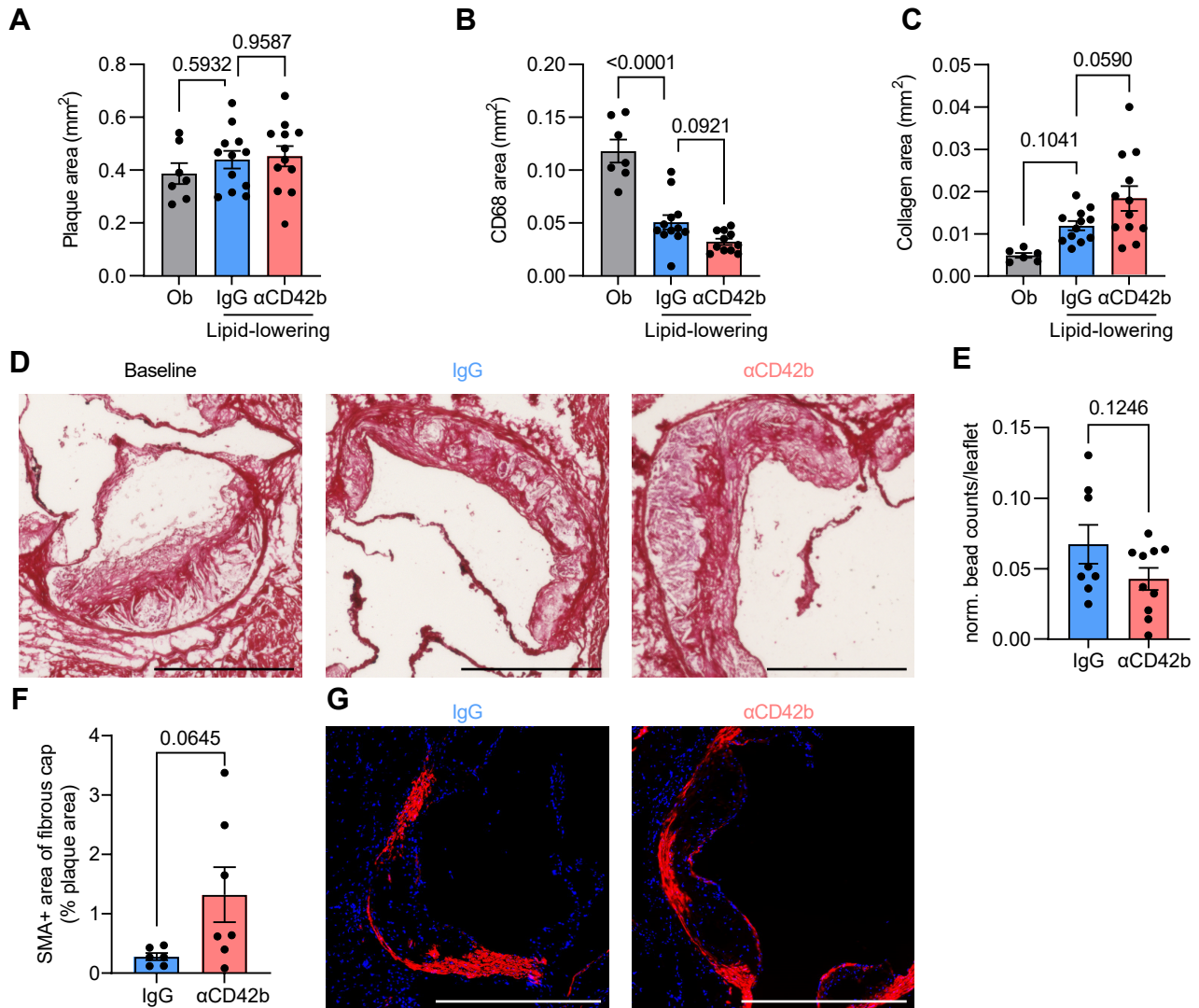
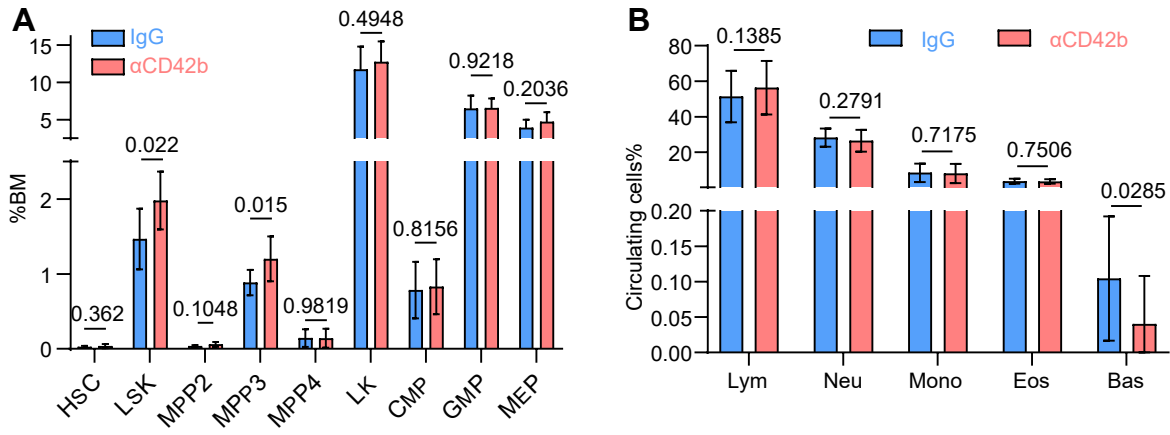


Supplemental Figure 1. Impaired glucose tolerance and platelet activation are sustained during the lipid-lowering period in diet-induced obese and atherosclerotic *Ldlr*^{-/-} male mice. (A) Weights (Lean n=14, Ob n=13, IgG n=17, αCD42b n=17) and (B) plasma cholesterol levels of Lean, Ob, IgG, αCD42b mice at harvest. (C) Gating strategy and (D) quantification of CD41+ cells in circulating blood of Ob, IgG and αCD42b mice three days before harvest. (E) Fasting glucose and (F) fasting insulin levels. (G) HOMA-IR calculations and (H) QUICKI quantification of Lean, Ob, IgG, αCD42b mice. In A, error bars represent SDs. Data in A and B were analyzed by Two-way ANOVA Dunnett's post hoc and One-way ANOVA Tukey's post hoc test, respectively. Data in D were analyzed by One-way ANOVA Sidak's post hoc test. Data in E, F and H were analyzed by One-way ANOVA Dunnett's post hoc test. Data in G were analyzed by One-way ANOVA Dunn's post hoc test. p-values are shown in graphs.

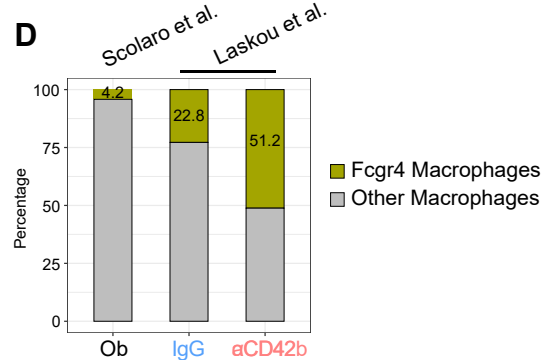
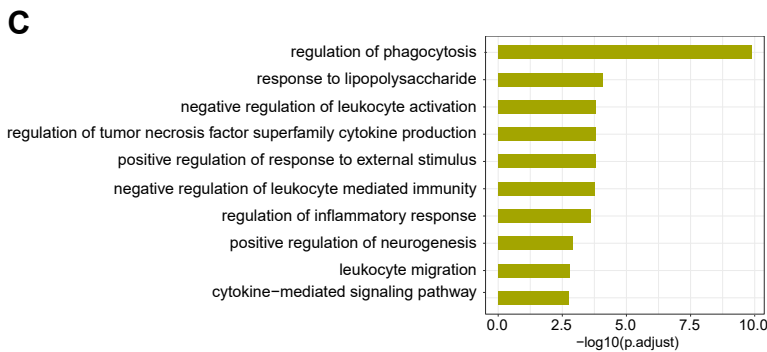
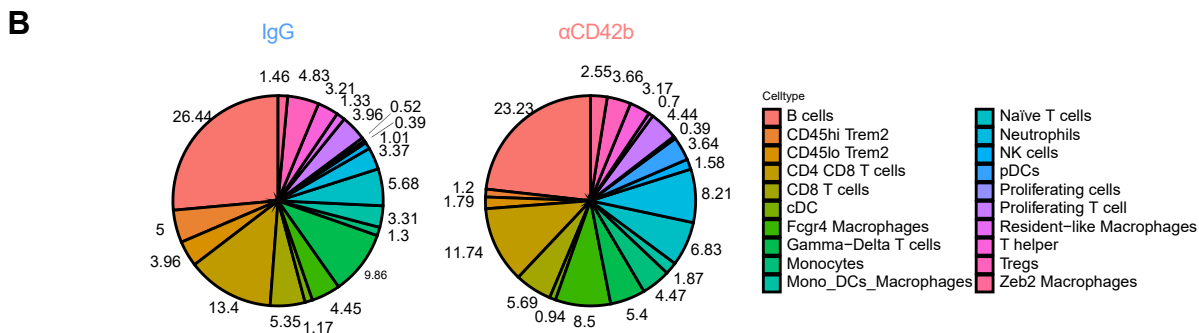
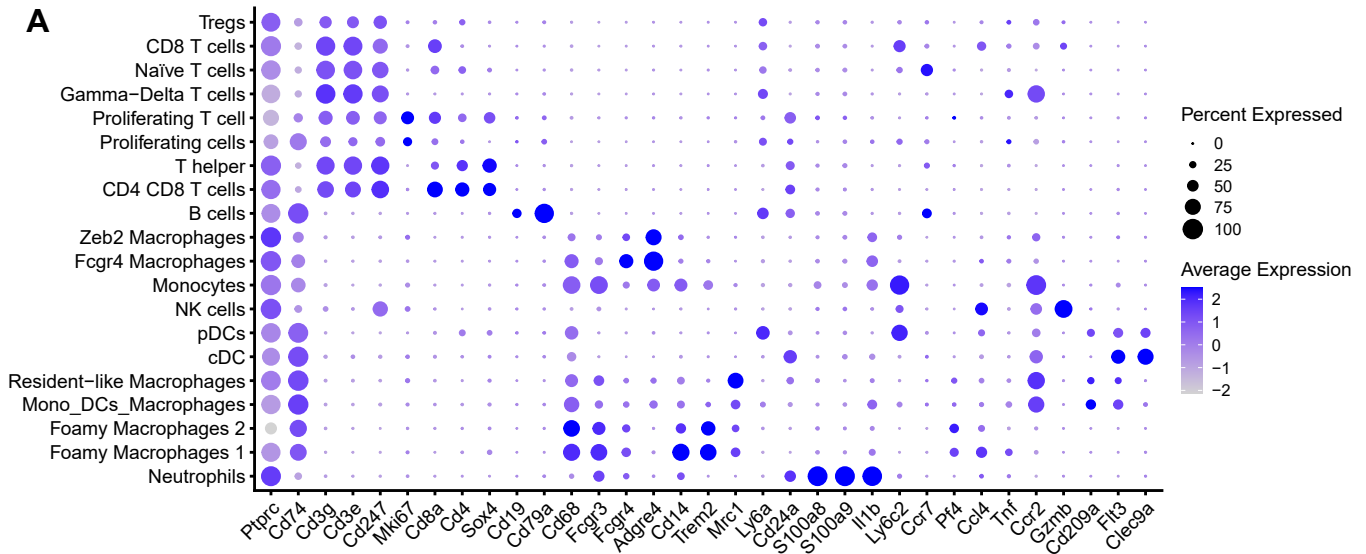


Supplemental Figure 2. Platelet deficiency alters plaque composition after lipid-lowering.

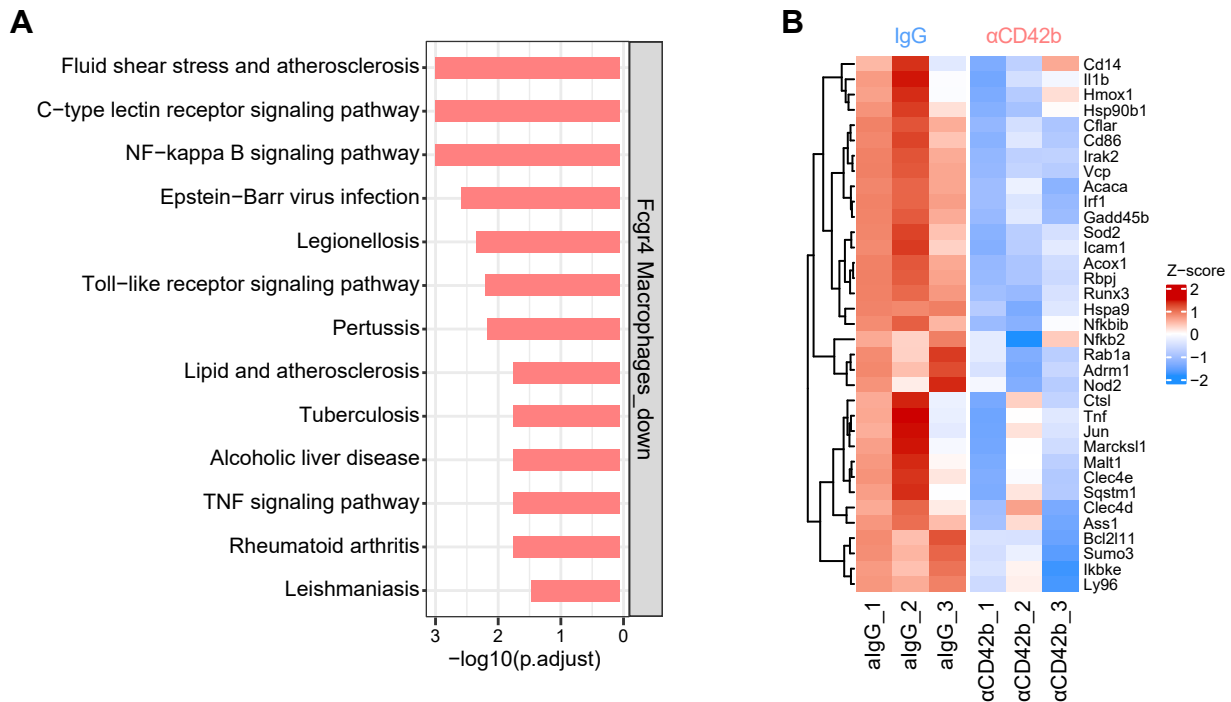
(A) Quantification of plaque burden (mm²) of aortic roots from Ob, IgG- and αCD42b-treated mice. (B) Quantification of immunohistochemical staining for CD68 area (mm²) in aortic root plaques of Ob, IgG- and αCD42b-treated mice. (C) Quantification of collagen area (mm²) in aortic root plaques of Ob, IgG- and αCD42b-treated mice and (D) brightfield representative images (scale bar=0.5mm). (E) Normalized bead counts of monocytes recruited in aortic root plaques of IgG- and αCD42b-treated mice. (F) Representative images and (G) quantification of SMA⁺ area of fibrous cap from IgG- or αCD42b-injected mice. Data in A, B, C and E, F were analyzed by One-way ANOVA Sidak's post hoc test and unpaired Student t-test, respectively. p-values shown in graphs.



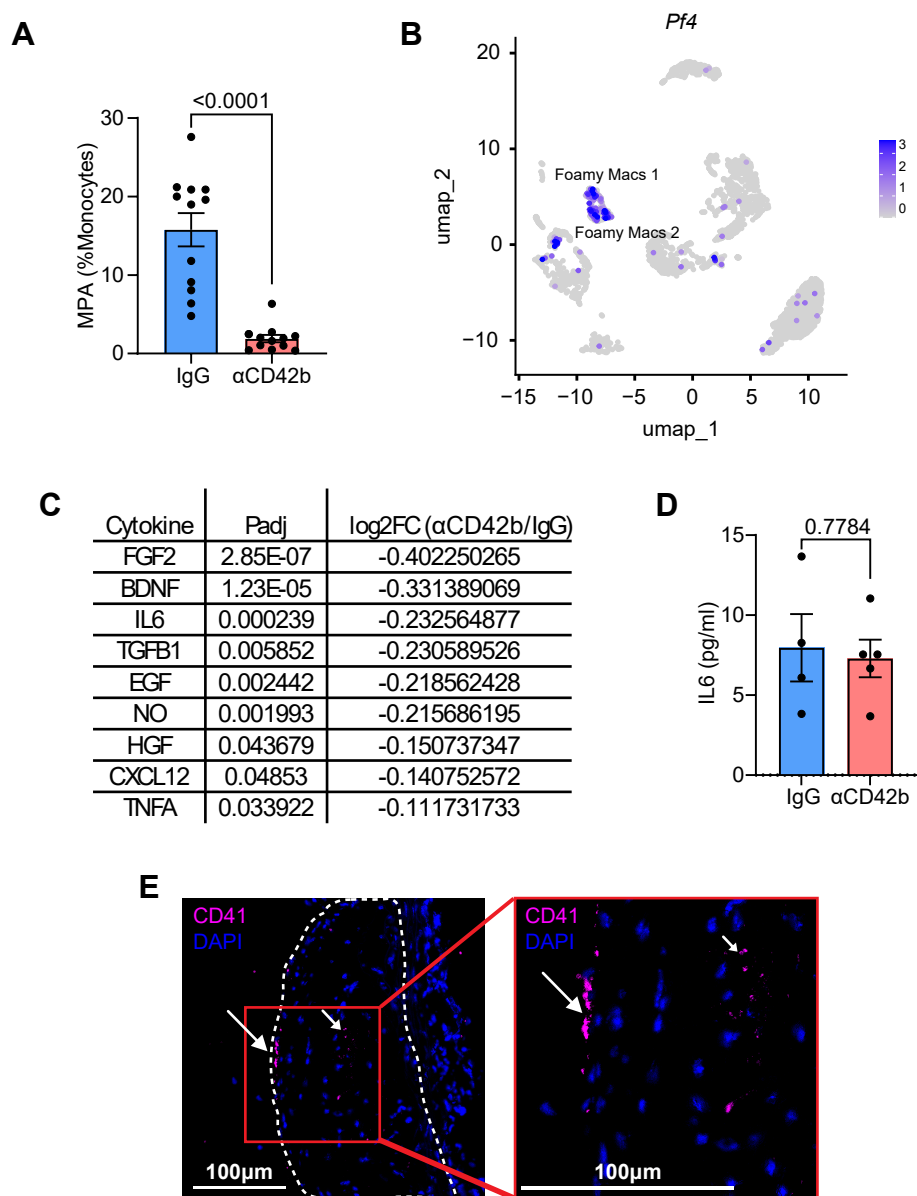
Supplemental Figure 3. Circulatory white blood cells and bone marrow progenitors in IgG- and α CD42b-treated mice. (A) Bone marrow progenitor cells and (B) white blood cells in circulation from IgG and α CD42b-treated mice. Data in A and B were analyzed by unpaired Mann Whitney. p-values shown in graphs.



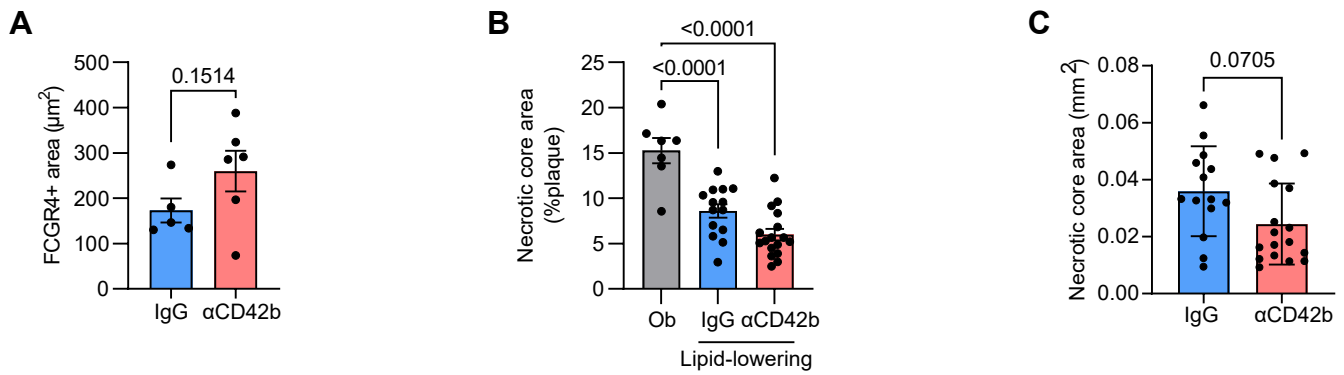
Supplemental Figure 4. CD45⁺ scRNA seq of platelet depleted mice reveals an increase in *Fcgr4*⁺ phagocytic macrophages and downregulation of inflammatory pathways after atherosclerosis inflammation resolution. (A) Heatmap showing normalized scaled expression of marker genes used to identify 20 cell types in leukocyte single-cell RNA-seq. **(B)** Proportion analysis of all clusters. **(C)** Top 10 most significantly overrepresented GO terms found among the top 100 marker genes of *Fcgr4*⁺ macrophage cluster. **(D)** Percentage of *Fcgr4*⁺ macrophages identified among all macrophages in αCD42b-treated mice, IgG-treated mice, and baseline obese (Ob) mice obtained from Scolaro et al. (24).



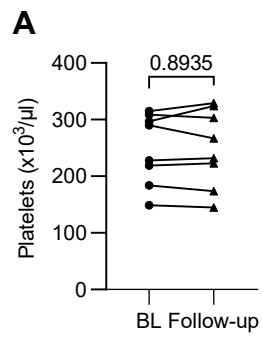
Supplemental Figure 5. CD45⁺ scRNA seq of platelet depleted mice reveals a downregulation of inflammatory pathways in *Fcgr4*⁺ macrophages during lipid-lowering. (A) Overrepresented KEGG terms (q-value<0.05) found among significantly downregulated genes in α CD42b relative to IgG samples in *Fcgr4*⁺ macrophage cluster. **(B)** Normalized scaled expression of genes that are associated with overrepresented KEGG terms shown in Suppl. Figure 4A. All pathways are significantly downregulated in α CD42b-treated mice relative to IgG-treated mice in *Fcgr4*⁺ macrophage cluster. In **A** and **B**, p-value < 0.05 and $|\log_2$ fold change| \geq 0.6, were used.



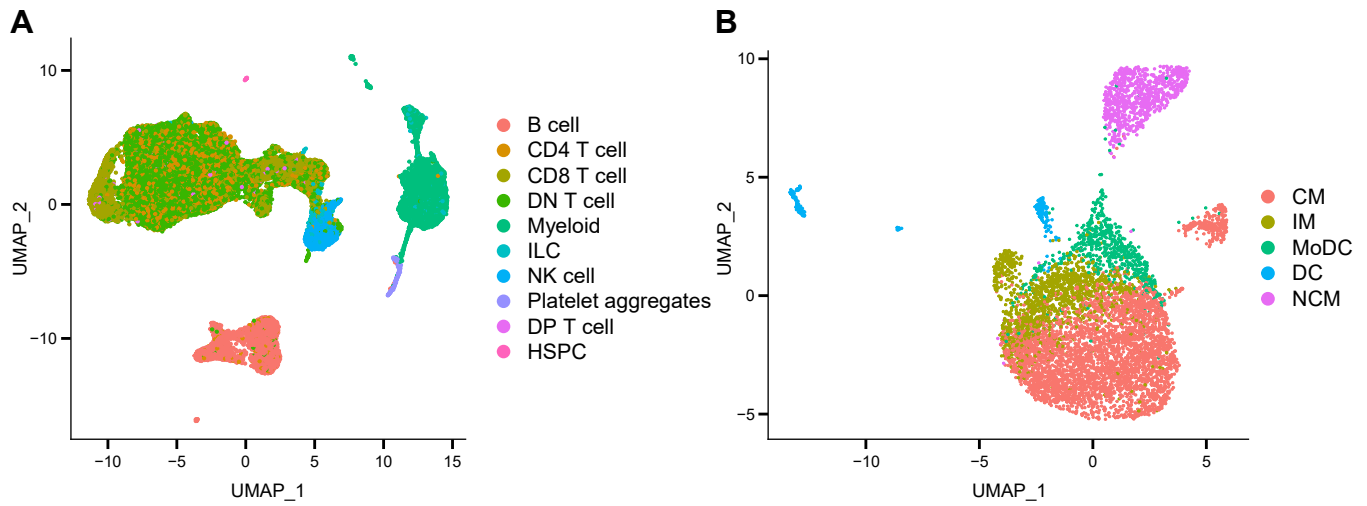
Supplemental Figure 6. Possible mechanisms for the effects of platelets on plaque myeloid cells after lipid-lowering. (A) Monocyte-Platelet aggregates in circulation of IgG- and α CD42b-treated mice. (B) UMAP of *Pf4*⁺ cells in CD45⁺ sequenced plaque cells. (C) Platelet-related upstream mediators in α CD42 compared to control IgG-treated mice. (D) Plasma IL6 levels from IgG- and α CD42b-treated mice. (E) CD41⁺ staining in atherosclerotic plaques from obese baseline mice. The arrow at the left points to the EC layer; that on the right is inside the plaque. Data in D were analyzed by unpaired Student t-test.



Supplemental Figure 7. During lipid-lowering, platelet depletion leads to increased abundance of FCGR4⁺ macrophages and reduces necrotic core content in plaques. (A) Quantification of FCGR4⁺ area in aortic root plaques of IgG- and αCD42b-treated mice. **(B)** Necrotic core content (%) of Ob, IgG- and αCD42b-treated mice. **(C)** Quantification of necrotic core areas in aortic root plaques of IgG- and αCD42b-treated mice. Data in **A** and **B** were analyzed by unpaired Student t-test or One-way ANOVA Sidak's post hoc test, respectively. Data in **C** were analyzed by unpaired Mann Whitney. p-values shown in graphs.



Supplemental Figure 8. Lipid-lowering treatments do not affect platelet counts in individuals with T2D. (A) Circulating platelet counts at baseline and follow-up in individuals with T2D from the CHORD study (n=8). Data in A were analyzed by a paired Student's t-test.



Supplemental Figure 9. PBMC scRNA-seq from subjects enrolled in the CHORD study. (A) UMAP of sequenced PBMCs from individuals enrolled in the CHORD study (n=6). **(B)** UMAP of sub-clustered myeloid cells from sequenced PBMCs from individuals, enrolled in the CHORD study (n=6).